

Sensitive Electrochemical Detection of Telomerase Activity Using Spherical Nucleic Acids Gold Nanoparticles Triggered Mimic-Hybridization Chain Reaction Enzyme-Free Dual Signal Amplification

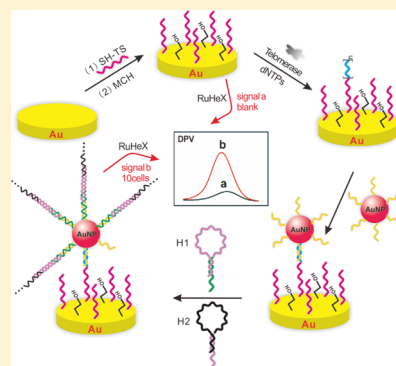
Wen-Jing Wang,[†] Jing-Jing Li,[§] Kai Rui,[†] Pan-Pan Gai,[†] Jian-Rong Zhang,^{*,†,‡} and Jun-Jie Zhu^{*,†}

[†]State Key Laboratory of Analytical Chemistry for Life Science, School of Chemistry & Chemical Engineering, Nanjing University, Nanjing 210093, People's Republic of China

[‡]School of Chemistry and Life Science, Nanjing University Jinling College, Nanjing 210089, People's Republic of China

[§]Department of Radiology, Affiliated Hospital of Xuzhou Medical College, Xuzhou 221006, People's Republic of China

ABSTRACT: We report an electrochemical sensor for telomerase activity detection based on spherical nucleic acids gold nanoparticles (SNAs AuNPs) triggered mimic-hybridization chain reaction (mimic-HCR) enzyme-free dual signal amplification. In the detection strategy, SNAs AuNPs and two hairpin probes were employed. SNAs AuNPs as the primary amplification element, not only hybridized with the telomeric repeats on the electrode to amplify signal but also initiated the subsequent secondary amplification, mimic-hybridization chain reaction of two hairpin probes. If the cells' extracts were positive for telomerase activity, SNAs AuNPs could be captured on the electrode. The carried initiators could trigger an alternative hybridization reaction of two hairpin probes that yielded nicked double helices. The signal was further amplified enzyme-free by numerous hexaammineruthenium(III) chloride ($[\text{Ru}(\text{NH}_3)_6]^{3+}$, RuHex) inserting into double-helix DNA long chain by electrostatic interaction, each of which could generate an electrochemical signal at appropriate potential. With this method, a detection limit of down to 2 HeLa cells and a dynamic range of 10–10 000 cells were achieved. Telomerase activities of different cell lines were also successfully evaluated.



Telomeres are known as “caps” of the eukaryotic chromosome end. They protect the regions of the chromosome end from fusion or degradation using their DNA–protein complex.¹ Cell division will shorten the length of the telomere, eventually cellular senescence and apoptosis occur when a critical telomere length is reached.^{2,3} Telomerase is a ribonucleoprotein that can maintain telomere length by adding repetitive nucleotide sequences (TTAGGG for vertebrates) onto the 3' ends of the chromosome using its intrinsic RNA template and reverse transcriptase.^{4–6} This property of telomerase is hypothesized the reason why cancer cells divide indefinitely, since over 85% of all known cancer cells overexpress telomerase while there is no detectable telomerase activity in normal cells.⁷ Therefore, telomerase is regarded as a valuable biomarker for cancer diagnosis as well as a therapeutic target.^{8,9} The evaluation of telomerase activity is of significant importance to the identify and therapy of cancer.

The most powerful and widely used method to determine telomerase activity in cell extracts and tissues is polymerase chain reaction (PCR)-based telomeric repeat amplification protocol (TRAP) and its modified assays.^{10–14} Although the sensitivity is ultrahigh with the help of PCR amplification, the disadvantages are also obvious, for example, the complicated manipulations. Additionally, the method is susceptible to PCR-derived artifacts.¹² The activity of Taq polymerase used in PCR is easily inhibited by concentrated cell extracts and it is unable to determine telomerase inhibition by quadruplex ligands.¹⁵ To

solve these problems, several kinds of PCR-free methods have been developed recently, including colorimetric,^{16,17} fluorescence,^{18,19} and chemiluminescence-based approaches.²⁰ All of them provide useful platforms for the detection of telomerase activity and related research, but they usually suffer from insufficient sensitivity and narrow detection range. In order to further develop these methods, nanoparticle-based^{21,22} and enzyme-based amplification^{23,24} have been introduced to the detection system. However, the possibility of practical application is hampered due to the high cost and complicated manipulation of protein enzyme. Other PCR-free methods to valid telomerase activity such as surface plasma resonance (SPR),²⁵ droplet digital PCR (ddPCR),²⁶ and so on suffer from the requirement of expensive and sophisticated instruments. Electrochemical technology is becoming more recognized in analyzing telomerase activity due to its own merits of high sensitivity, simplified setup, low cost.^{27–29} To further enhance the detection sensitivity, approaches for background decrease or signal amplification are commonly considered. Enzyme exonuclease III has been employed to decrease the background signal,^{30,31} but protein enzyme has its own shortcomings of making the detection relatively costly and complicated. Thus,

Received: December 15, 2014

Accepted: February 11, 2015

Published: February 11, 2015



an alternative strategy to amplify the signal is still urgently needed.

Hybridization chain reaction (HCR) is an enzyme-free, room temperature linear amplification approach which is simple in operation and cost-effective only using the DNA single strand.³² Two DNA hairpin probes can stably coexist in the hybridization solution. However, the introduction of initiators will trigger an alternating hybridization of two probes into nicked double helices. Since proposed, it has been widely used in amplified detection of DNA,³³ microRNA,³⁴ small molecule,³⁵ protein,³⁶ and cells³⁷ and has achieved a series of satisfactory results. However, HCR has not been found for the use of telomerase detection.

Herein, we adapt HCR enzyme-free amplification to detect telomerase activity by means of electrochemical technology. In order to improve the sensitivity, spherical nucleic acids gold nanoparticles (SNAs AuNPs), which have been widely used for signal amplification,^{38,39} are introduced into the detection system as primary amplification element. Once the telomeric repeats are formed on the electrode, SNAs AuNPs can be captured. For the specific initiator on the AuNP, we design two hairpin probes that can alternate hybridization to form a nicked double helix like HCR in the presence of initiator, while partly self-hybridize in the absence of initiator on the contrary to HCR. We call this reaction as mimic-HCR and it works as a secondary amplification element, which is demonstrated to have the same amplifying function like HCR. Subsequent static insertion of RuHex into the nicked double helices can generate an amplified electrochemical signal. The dual signal amplification strategy of the SNAs AuNPs triggered mimic-HCR is proved to be a sensitive, simple method for the evaluation of telomerase activity in cell extracts.

EXPERIMENTAL SECTION

Chemicals and Materials. 3-[(3-Cholamidopropyl)-dimethylammonio]-1-propanesulfonic acid (CHAPS), tris(2-carboxyethyl)phosphine hydrochloride (TCEP), Tween 20, 6-mercaptop-1-hexanol (MCH), and hexaammineruthenium(II) chloride ($[\text{Ru}(\text{NH}_3)_6]^{3+}$, RuHex) were purchased from Sigma-Aldrich (St. Louis, MO). Ethylene glycol bis(aminoethyl ether)-*N,N,N',N'* tetraacetic acid (EGTA), phenylmethylsulfonyl fluoride (PMSF), glycerol, deoxynucleotide triphosphates (dNTPs) solution mixture, 40% acrylamide mix solution, ammonium persulfate (APS), 1,2-bis(dimethylamino)-ethane (TEMED), and low range DNA ladder were obtained from Sangon Biotechnology Co. Ltd. (Shanghai, China). The PCR kit was purchased from Beyotime Institute of Biotechnology (Haimen, China).

All the oligonucleotides used here were synthesized and purified by Sangon Biotechnology Co. Ltd. (Shanghai, China), and all the oligonucleotide sequences are listed in Table 1. A 0.1 M PBS (pH 7.4) buffer was used as the immobilization buffer (Buffer I). A 0.1 M PBS (pH 7.4) buffer containing 0.5 M NaCl was employed as mimic-HCR buffer and washing buffer (Buffer II). A 10 mM Tris-HCl (pH 7.4) containing 5 μM $[\text{Ru}(\text{NH}_3)_6]^{3+}$ buffer was used as the electrochemical buffer (Buffer III). A 0.1 M PBS (pH 7.4) buffer containing 10 mM $\text{Fe}(\text{CN})_6^{3-}/\text{Fe}(\text{CN})_6^{4-}$ and 1 M KCl was used as the electrochemical impedance spectroscopy (EIS) buffer. All other chemicals were of analytical grade and were used as received without any purification. All the water used in the work was RNase-free.

Table 1. Probes and Sequences of the Oligonucleotides Used in This Study

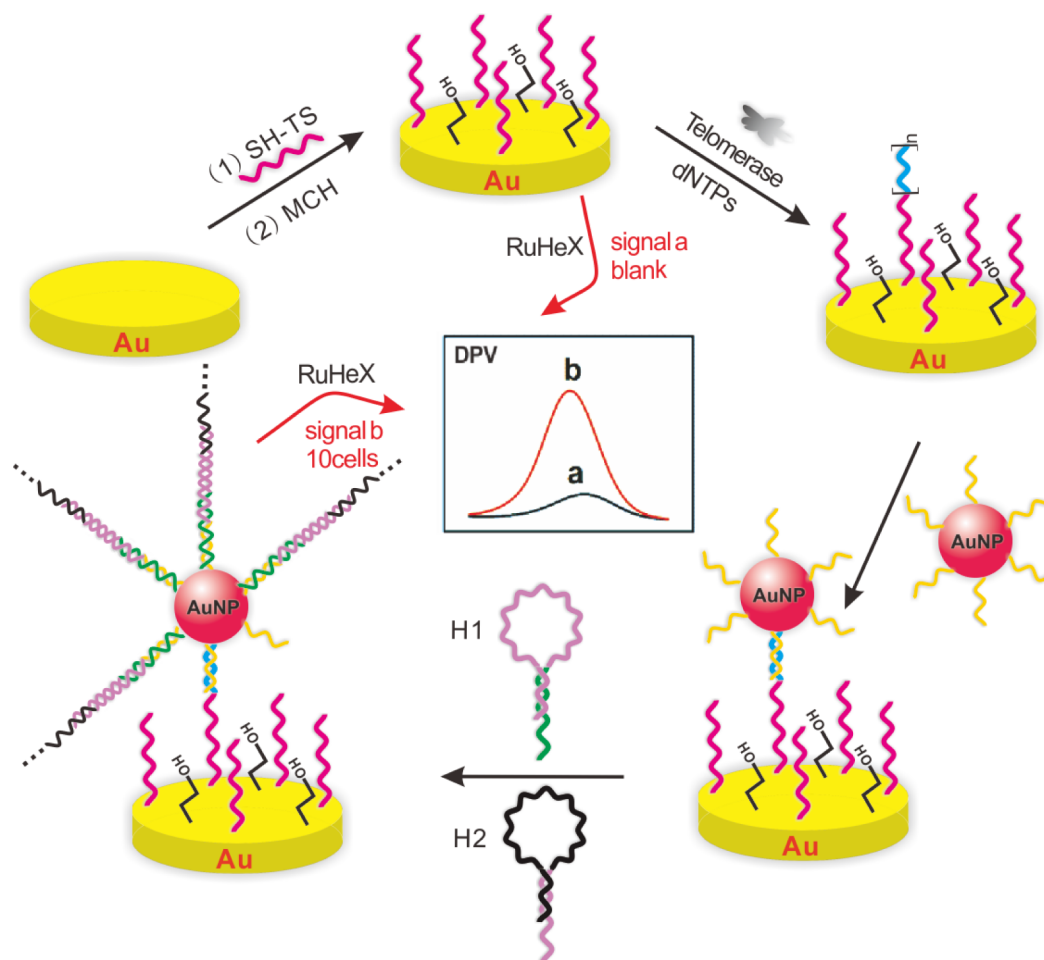
Name	Sequence (5'-3')
TS	AATCCGTCGAGCAGAGTT
SH-TS	SH-(CH ₂) ₆ -TTTTTTAATCCGTCGAGCAGAGTT
ACX	GCGCGGCTTACCCTTACCCTTACCCTTACC
SH-comple-10T	SH-(CH ₂) ₆ -TTTTTTTTTCCCTAACCCCTAACCCCTAA
H1	CCCTAACCCCTAAGTAGTGTAGGGTTAGGGTTAGGG
H2	CACTACTTAGGGTTAGGGCCCTAACCCCTAACCCCTAA
H3	AGGGTTAGGGTTGTGATGAACCCCTAACCCCTAACTCT
H4	CATCACAACCCCTAACCCCTAGAGTTAGGGTTAGGGTT

Cell Culture and Telomerase Extraction. HeLa cells, A549 cells, MCF-7 cells, and MDA-MB-231 cells were seeded in DMEM medium (Gibco, Grand Island, NY) supplemented with 10% fetal calf serum (Gibco, Grand Island, NY), penicillin (100 $\mu\text{g}/\text{mL}$), and streptomycin (100 $\mu\text{g}/\text{mL}$) in 5% CO₂, 37 °C incubator. K562 cells were cultured in RPMI-1640 medium (Gibco, Grand Island, NY) supplemented with 10% fetal calf serum (Gibco, Grand Island, NY), penicillin (100 $\mu\text{g}/\text{mL}$), and streptomycin (100 $\mu\text{g}/\text{mL}$) in 5% CO₂, 37 °C incubator. All kinds of cells were collected in the exponential phase of growth, and 1 million cells were dispensed in a 1.5 mL EP tube, washed twice with ice-cold phosphate buffered saline (pH 7.4) solution, and resuspended in 200 μL of ice-cold CHAPS lysis buffer (10 mM Tris-HCl, pH 7.5, 1 mM MgCl₂, 1 mM EGTA, 0.5% (w/v) CHAPS, 10% (v/v) glycerol, 0.1 mM PMSF). The cells were incubated for 30 min on ice and then centrifuged for 20 min (12 000 rpm, 4 °C). Without disturbing the pellet, the cleared lysate was carefully transferred to a fresh RNase-free tube, flash frozen, and stored at -80 °C before use.

TRAP Assay for Telomerase Activity. The telomerase extracts (40 μL) were added to 10 μL of extension solution containing TRAP buffer (20 mM Tris-HCl, pH 8.3, 1.5 mM MgCl₂, 63 mM KCl, 0.005% (v/v) Tween 20, 1 mM EGTA), 1 mM dNTPs, and 200 nM TS primer. The solution was incubated at 30 °C for 60 min. For negative control experiments, telomerase extracts were heated at 95 °C for 10 min. A volume of 1 μL (2 μL) of telomerization products were added into 49 μL (48 μL) of solution which contains 1 \times PCR buffer, 200 μM dNTPs, 3 U of Taq DNA polymerase, 0.1 μg of TS primer, and 0.1 μg of ACX primer. PCR was carried out with the GeneAmp PCR System 9700 by the following program: 94 °C for 4 min; 30 cycles at 94 °C for 30 s, 58 °C for 30 s, and 72 °C for 30 s; 72 °C for 5 min; 4 °C hold. A 12% polyacrylamide gel was employed here for the verification of telomerase activity, and 15 μL of PCR products were loaded on the gel. Electrophoresis was carried out at 100 V for 80 min at room temperature in 1 \times TBE buffer. After separation, the gel was stained by ethidium bromide and imaged with the fluorescence gel imaging system.

Preparation of Spherical Nucleic Acids (SNAs) AuNPs. Citrate-capped AuNPs (13 nm) were prepared according to the literature procedure.⁴⁰ Briefly, 10 mL of 38.8 mM trisodium

Scheme 1. Schematic Illustration of SNAs AuNPs Triggered Mimic-HCR Dual Signal Amplification Electrochemical Assay for Telomerase Activity Detection



citrate was added to a boiling solution with 100 mL of 1 mM HAuCl_4 under vigorous stirring. Within several minutes, the color of the solution changed from pale yellow to deep red. The mixture was allowed to heat for 15 min under reflux, another 15 min at room temperature, then slowly cooled to room temperature, and finally stored at 4 °C until use. SNAs AuNPs were prepared as reported previously.⁴⁰ A volume of 6 μL of 250 μM SH-comple-10T primer was activated by 1.5 μL of 100 mM TCEP at pH 5.2 for 1 h. The activated DNA was then mixed with 500 μL of AuNPs. After incubation for 16 h at room temperature, the colloid solution was salted to 0.1 M NaCl by adding 50 μL of 1 M NaCl and allowed to stand for 24 h. To remove excess DNA, the solution was purified by centrifuging for 30 min at 12 000 rpm four times. SNAs AuNPs were finally redispersed in Buffer II and stored at 4 °C for further use.

Electrode Pretreatment. The 2 mm diameter gold electrode (CH Instruments Inc., Shanghai, China) was polished with various particle sizes (1, 0.3, and 0.05 μm) alumina slurry to obtain a mirror-like surface and washed by sonication in ethanol and ultrapure water for 5 min each to remove residual alumina powder. The electrode was electrochemically cleaned by cycling the potential between -0.2 and $+1.5$ V (at a scan rate of 0.1 V/s) in a fresh 0.5 M H_2SO_4 until a stable cyclic voltammogram was obtained. The cleaned gold electrode was rinsed with a copious amount of RNase-free water and blown dry with nitrogen.

Fabrication of Sensors. To each pretreated working electrode, 5 μL of various concentrations of SH-TS primer in Buffer I was added and incubated for 2 h. The surface was washed by RNase-free water and subsequently immersed into 1 mM MCH (in water) solution for 1 h, then washed by RNase-free water again. The electrode was dipped in 20 μL of extension solution containing a different number of cells, 1 \times TRAP buffer (20 mM Tris-HCl, pH 8.3, 1.5 mM MgCl_2 , 63 mM KCl, 0.005% (V/V) Tween 20, 1 mM EGTA), 1 mM dNTPs for 1 h at 37 °C, followed by a thorough rinse with RNase-free water. A volume of 10 μL of SNAs AuNPs (in Buffer II) solution was dropped on a gold electrode and incubated for 90 min at room temperature. After washing with Buffer II, a droplet of 10 μL solution containing 1 μM H1 and 1 μM H2 was cast onto the surface for another 90 min, washing the electrode with Buffer II for electrochemical measurement.

Electrochemical Characterization and Measurements. All the measurements were performed using a conventional three-electrode system with an Ag/AgCl (3 M KCl) reference electrode, a Pt counter electrode, and the working electrode of modified gold electrode. EIS analysis was carried out on an Autolab PGSTAT12 (Ecochemie, BV, The Netherlands) in EIS buffer with the frequency range of 10^{-1} to 10^5 Hz, 5 mV amplitude. Electrochemical measurements were performed on a CHI 660D workstation (CH Instruments Inc., Shanghai, China) in Buffer III. The electrochemical signal was measured with differential pulse voltammetry (DPV) by scanning from

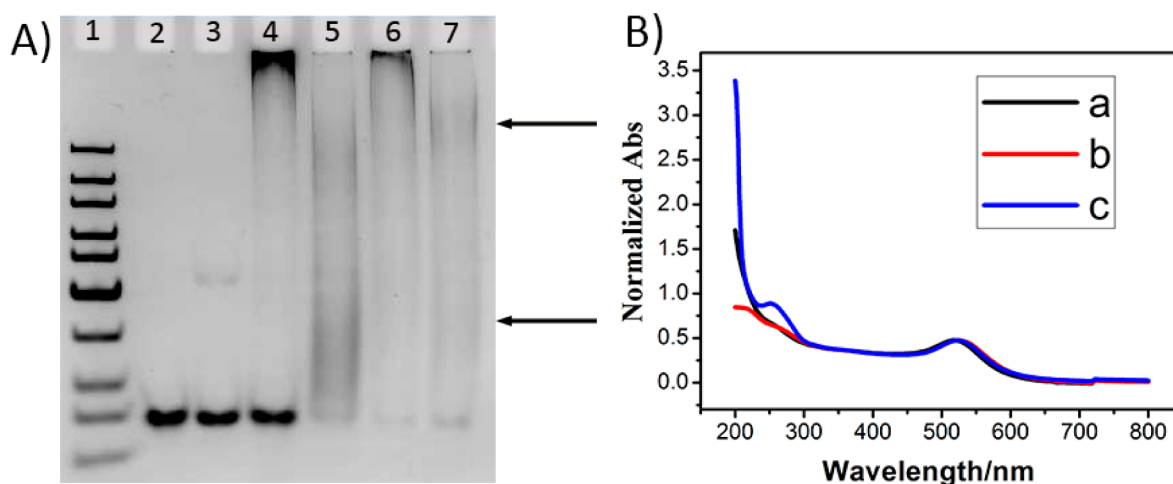


Figure 1. (A) EB-stained 12% polyacrylamide gel electrophoresis (PAGE) image. Lane 1, low range DNA ladder; Lane 2, 1 μ M H1; Lane 3, 1 μ M H2; Lane 4, 1 μ M H1 + 1 μ M H2; Lane 5, 1 μ M H1 + 1 μ M H2 + 1 μ M SH-comple-10T initiator strands; Lane 6, 1 μ M H1 + 1 μ M H2 + 1 μ M SNAs AuNPs; Lane 7, Lane 6 after treatment with 10 mM DTT for 1 h (all the samples were mixed and incubated at room temperature for 1 h); (B) UV-vis absorption spectra of (a) 13 nm AuNPs, (b) SNAs AuNPs, and (c) SNAs AuNPs after mimic-HCR with 1 μ M H1 and 1 μ M H2 for 1 h.

+0.2 to −0.6 V (versus Ag/AgCl) in 3 mL of Buffer III solution, which was degassed with nitrogen for 15 min.

RESULTS AND DISCUSSION

Design and Characterizations of the Sensor. The principle of SNAs AuNPs triggered mimic-HCR dual signal amplification enzyme-free electrochemical assay for telomerase activity detection is shown in Scheme 1. Three parts were mainly involved in the assay: (i) telomerase primer was extended on the electrode; (ii) SNAs AuNPs were captured to initiate mimic-HCR for dual signal amplification; (iii) electrochemical detection was performed in RuHex solution. In the first part, thiol-modified telomerase primers were immobilized on the gold electrode and extended by telomerase in cell extracts to form telomeric repeats (TTAGGG)_n. In the second part, SNAs AuNPs were introduced to hybridize with telomeric repeats as the primary amplification element owing to the larger surface area of the AuNP with numerous DNA. At the same time, numerous DNA strands on AuNP acted also as initiators to trigger mimic-HCR to further amplify the signal. With the help of these two steps, the electrochemical signal for the detection of telomerase could be amplified remarkably. The 5'-end thiol-modified SH-comple-10T DNA sequences were immobilized on 13 nm gold nanoparticle to form SNAs AuNPs. The (CCCTAA)₃ sequence in SH-comple-10T DNA was complementary to three telomeric repeats, which could be used to capture SNAs AuNPs on the electrode and then initiated mimic-HCR. For SH-comple-10T DNA sequences initiators on AuNP, two hairpin probes Hairpin 1 (H1) and Hairpin 2 (H2) were designed as shown in Table 1. Each hairpin has a stem of 12 base pairs enclosing a hexanucleotide loop and an additional hexanucleotide sticky end at the 3' end of H1 (complementary to the loop of H2) as well as at the 5' end of H2 (complementary to the loop of H1). In the presence of initiator, H1 would be opened since the initiator could recognize the sticky end of H1 and undergo a strand displacement reaction to hybridize with the green fragment of H1 in Table 1. In the same way, H2 would be opened since the newly exposed fragment of H1 could recognize the sticky end of H2 and undergo a strand displacement reaction to hybridize with the purple fragment of H2. The black fragment of H2 was

the same with an initiator. Thus, a cascade of hybridization events between the two hairpin probes could happen on AuNP to form a nicked double-helix and amplify the signal of initiator binding just like HCR on the electrode. However, there was a little bit of a difference between this reaction and HCR due to the sequences' own specificity for telomeric repeat. In the absence of initiator, part of the two hairpin probes could also hybridize each other but could not be captured on the electrode. In the third part, the electrode was immersed in the RuHex solution. Numerous positive charged RuHex was gathered to negative charged DNA nicked double helices on the electrode via electrostatic interaction and eventually resulted in a remarkable amplified electrochemical signal. By monitoring the change of the electrochemical signal, we could indirectly determine the activity of telomerase with high sensitivity. Taking advantage of the high amplification efficiency of SNAs AuNPs triggered mimic-HCR enzyme-free dual signal amplification reaction, the proposed method could be used to economically, simply, and sensitively monitor the telomerase activity for clinical use.

The dual signal amplification was realized via SNAs AuNPs triggered mimic-HCR. To test the design, gel electrophoresis was used to characterize this process (Figure 1A). When mixing H1 (Lane 2) and H2 (Lane 3) together, part of them hybridized with each other to form a large molecular weight DNA complex at the top of the lane; meanwhile, a large amount of unreacted species was at the bottom of the lane (Lane 4). Once initiator strands were introduced into the mixture of H1 and H2, the unreacted species and the large molecular weight complex almost disappeared completely, indicating the successful initiation of the mimic-HCR (Lane 5). Then SNAs AuNPs were mixed with H1 and H2 to determine whether this reaction was still valid if initiators were immobilized onto AuNP. As shown in Lane 6, H1 and H2 were almost completely consumed, and the diffuse bands disappeared. Compared with initiator alone (Lane 5), large molecular weight complex were formed in Lane 6, which was ascribed to the production of mimic-HCR on the AuNP. After treating sample 6 with 10 mM DTT to destroy the Au–S bond, the reappearance of diffuse bands as those in Lane 5 further indicated that the mimic-HCR could be initiated on the AuNP

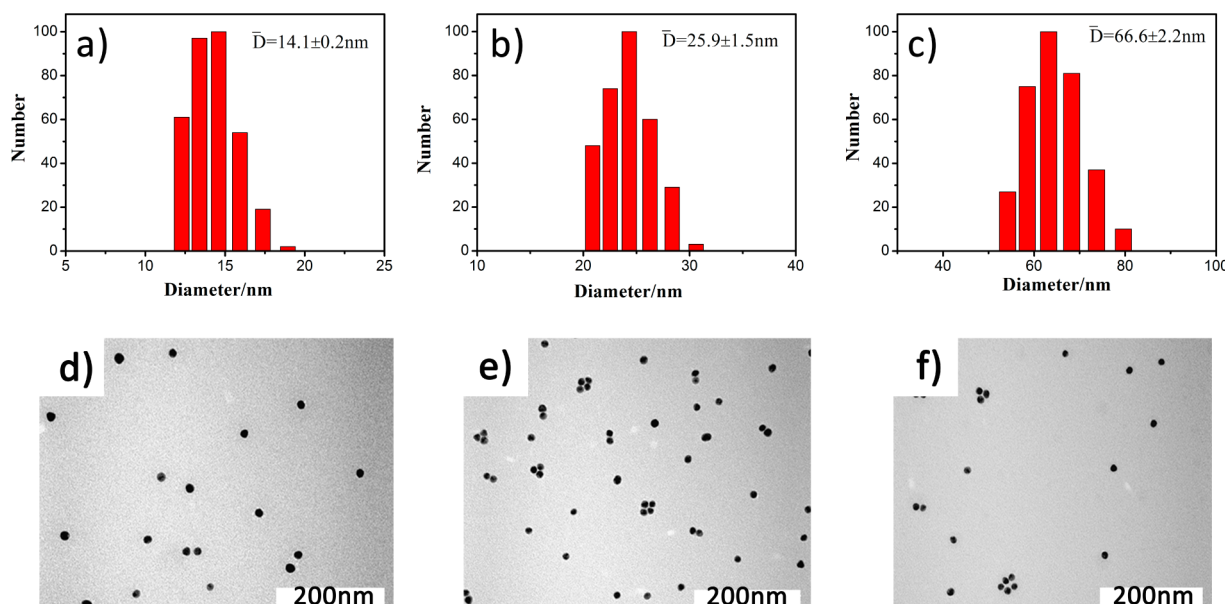


Figure 2. Average hydrodynamic sizes characterization by dynamic light scattering (DLS) and morphology characterization by transmission electron microscopy (TEM): (a and d) AuNPs, (b and e) SNAs AuNPs, (c and f) SNAs AuNPs after mimic-HCR with 1 μ M H1 and 1 μ M H2 for 1 h.

surface successfully (Lane 7). This result could also be confirmed by UV–vis absorption spectroscopy (Figure 1B). Two absorption peaks at 260 and 524 nm (curve c in Figure 1B) were observed in the UV–vis absorption spectroscopy of SNAs AuNPs after the mimic-HCR, but only one absorption peak at 524 nm could be observed in the absence of H1 and H2 (curve b in Figure 1B). This obvious absorption peak at 260 nm came from the linkage of H1 and H2 to the SNAs AuNPs.

In addition, the average hydrodynamic sizes of AuNPs were also determined to monitor this process. The hydrodynamic size of bare AuNPs solution was 14.1 ± 0.2 nm (Figure 2a), while it increased to 25.9 ± 1.5 nm for SNAs AuNPs after the immobilization of initiators on AuNP (Figure 2b). Once mixing with H1 and H2, the hydrodynamic size of SNAs AuNPs solution reached to 66.6 ± 2.2 nm (Figure 2c), confirming the increased size came from the DNA assembly, and this result was also similar to those that have been documented.⁴¹ At the same time, the morphology and dispersity of the AuNPs remained the same during this process as shown in Figure 2d–f. All the above results testified the feasibility of the design.

Electrochemical Characterization. EIS is a powerful electrochemical technique to monitor the assembly processes of the working electrode step by step. Figure 3 displayed the Nyquist plots to characterize the fabrication procedures of the electrode using $[\text{Fe}(\text{CN})_6]^{4-}/^{3-}$ as an electroactive probe. The bare gold electrode exhibited small impedance (Figure 3a), reflecting excellent conductivity. With the immobilization of SH-TS primer onto the electrode via a Au–S bond, the impedance was increased (Figure 3b), which was attributed to the strong electrostatic repulsion between the phosphoric acid groups of the DNA backbone and the negatively charged redox indicator ferricyanide. After the MCH blocking the left place on the gold electrode and replacing the noncovalent linked SH-TS primer, an obvious increase in the impedance signal was observed (Figure 3c). The elongation of the SH-TS primer led to a further increase of the impedance since more DNA bases were added to the electrode surface (Figure 3d). The impedance further increased after subsequent capture of SNAs AuNPs (Figure 3e), which resulted from numerous

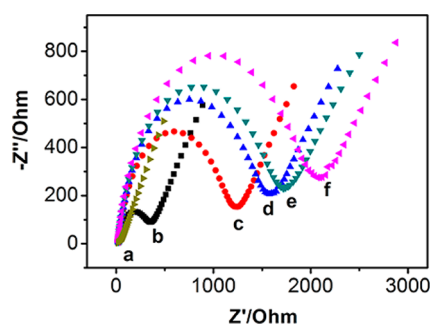


Figure 3. Electrochemical impedance spectra of bare gold electrode (a), SH-TS modified gold electrode (b), MCH blocked gold electrode (c), the extended SH-TS primer (d), capture of SNAs AuNPs (e), and mimic-HCR with H1 and H2 (f). The HeLa cell number was 2000.

negatively charged DNA strands on the AuNP repulsing electroactive indicator. Finally, SNAs AuNPs triggered mimic-HCR brought more DNA strands to the electrode surface resulting in a dramatic increase of the impedance (Figure 3f). Therefore, the enhancement of the impedance step by step confirmed the successful preparation of the biosensor well.

DPV Signal Behavior of the Biosensor. $[\text{Ru}(\text{NH}_3)_6]^{3+}$ (RuHex), which binds to anionic phosphate of DNA strands through electrostatic interaction, was used as the signal molecule in our study. The DPV amplified signal is shown in Figure 4. The signal of the blank electrode, which modified with SH-TS primer and MCH was weak (Figure 4a). After incubating the extended working electrode with another two designed hairpin probes (H3 and H4 in Table 1) for telomeric repeats, the signal increased to some extent (Figure 4b). Similarly, when SNAs AuNPs were incubated with the extended working electrode, the amplification effect was not so obvious (Figure 4c). However, once further incubated with H1 and H2, the signal increased remarkably (Figure 4d), demonstrating the dual amplification effect was quite efficient. Then we compared our fabricated method with the TRAP assay to verify the reliability. As shown in Figure 5, the result obtained from the as-fabricated biosensor was in accordance with that from

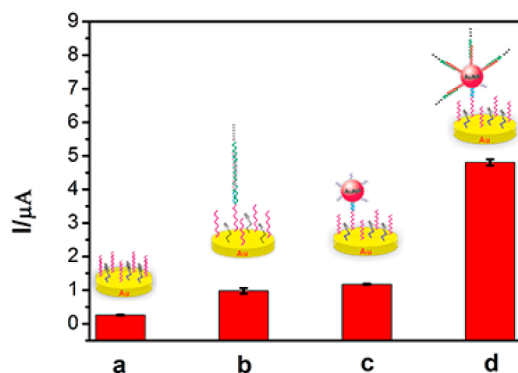


Figure 4. DPV signal behavior of blank electrode (a), one step amplification by mimic-HCR (b), one step amplification by capturing SNAs AuNPs (c), two step amplification by SNAs AuNPs triggered mimic-HCR with H1 and H2 (d). The HeLa cell number was 2000.

TRAP. With the TRAR assay, a six base-pair ladder could be observed for 1000 and 2000 cell extracts (Lane 1 and 2 in Figure 5b), indicating the activity of telomerase extracts, which corresponded to the obvious DPV signals (Figure 5a). By contrast, for cell lysis buffer and heated telomerase cell extracts, there was no significant band for the TRAR assay (Lane 3 and 4 in Figure 5b) and weak DPV signals were observed (Figure 5a). These results indicated the viability of the fabricated biosensor for the evaluation of telomerase activity.

Optimization of SH-TS Primer Concentration. The SH-TS primer concentration is the most important parameter for the performance of the proposed biosensor. In order to obtain high extended efficiency for telomerase and high hybridization efficiency for SNAs AuNPs in the following step, the probe concentration was optimized. As shown in Figure 6, with the increase of SH-TS primer concentration, a sharp increase in the DPV signal was observed from 0 to 0.5 μM, which came from the extension of more primer on the electrode. However, with the continuous increase of the concentration, the signal tended to decrease since more SH-TS primer on the electrode could hinder the extension effect of telomerase and the hybridization efficiency for SNAs AuNPs. Therefore, the optimized concentration of SH-TS primer used for electrode modification was 0.5 μM.

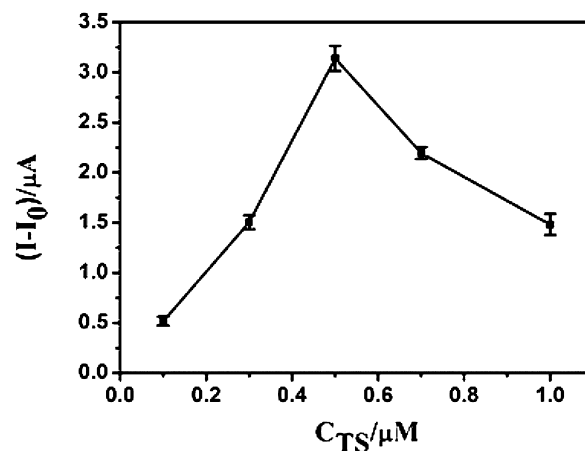


Figure 6. Optimization of SH-TS primer concentration used for electrode modification. The HeLa cell number was 1000.

Telomerase Activity Detection Using the Biosensor.

The telomerase activity of cell extracts was subsequently evaluated by the proposed approach to validate the sensitivity of this strategy. Cell extracts for telomerase were prepared as the literature reported previously.¹⁰ Figure 7a displays the DPV signal of biosensor corresponding to HeLa cells at different numbers. The DPV signal intensity increased monotonically with the logarithm no. of HeLa cells as shown in Figure 7b, and the inset showed that the signal from even 10 cells could be easily distinguished from the background. This method could realize the telomerase activity measurement down to 2 HeLa cells (S/N = 3), with the improved dynamic range from 10 to 10 000 HeLa cells. This result could be comparable with enzyme-based electrochemical and optical telomerase biosensors^{24,31} by enzyme-free amplification.

Evaluation Telomerase Activity of Different Cell Line.

To ensure the practicability, we evaluated five different cell lines using the proposed method. As shown in Figure 8, all of these cell lines were positive for telomerase activity, except for the heated HeLa cells sample, which showed a weak signal as background. As previously reported, the telomerase activity of HeLa and A549 cells was higher than that of MCF-7, K562, and

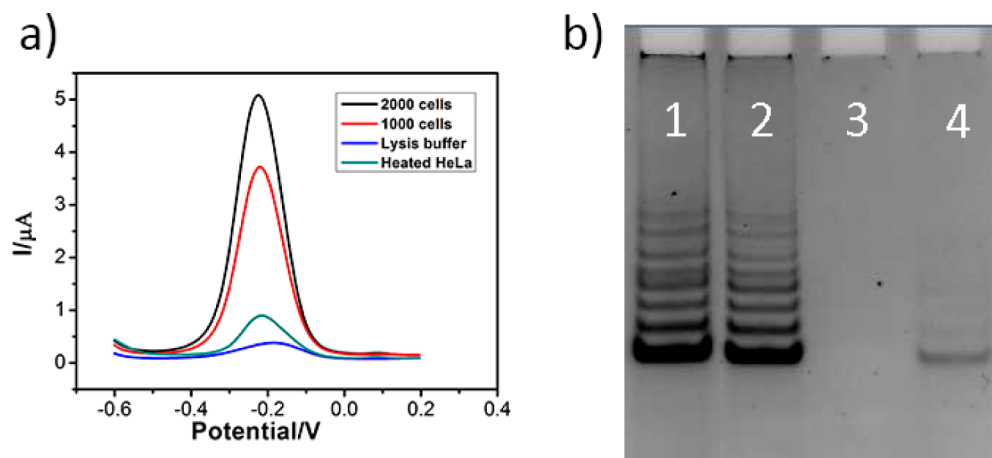


Figure 5. (a) DPV signals of different samples using SNAs AuNPs triggered mimic-HCR amplification electrochemical assay. (b) TRAP assay for different samples: Lane 1 and 2, cell extracts equivalent to 2000 and 1000 cells, respectively; Lane 3 and 4, lysis buffer only and heated 1000 cells extracts, respectively.

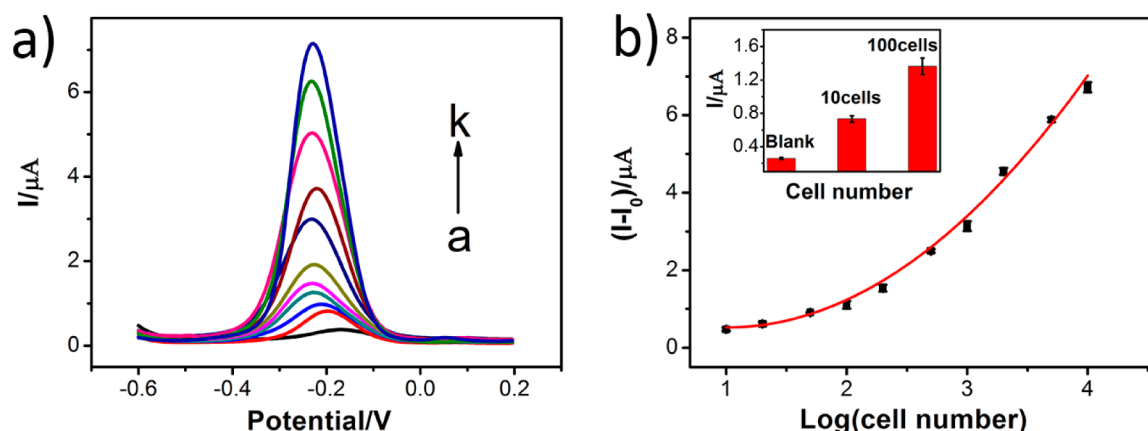


Figure 7. (a) DPV signals of a range of HeLa cell numbers. From bottom to top: 0, 10, 20, 50, 100, 200, 500, 1000, 2000, 5000, and 10 000 cells. (b) Logarithmic plot of current vs. HeLa cell numbers (10–10 000 cells). Inset shows the current signal from blank, 10, and 100 HeLa cells. The error bars represent standard deviations for measurements taken from at least three independent experiments.

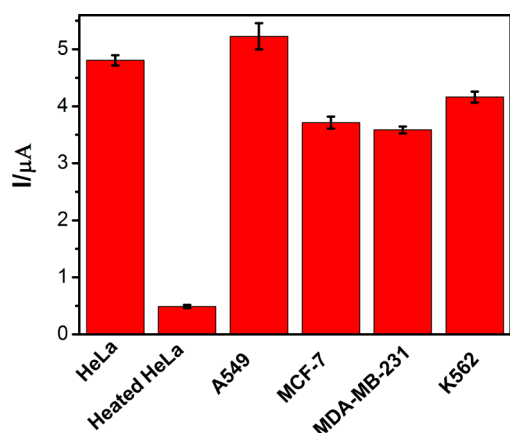


Figure 8. Evaluation of telomerase activity from different cell lines extracts. All the cell numbers were 2000.

MDA-MB-231 cells,^{17,42} indicating the reliability of our method.

CONCLUSIONS

We have developed an electrochemical assay to evaluate telomerase activity of cell extracts using SNAs AuNPs triggered mimic-HCR dual signal enzyme-free amplification. This method could detect telomerase activity as low as 2 HeLa cells, with a wide detection range from 10 to 10 000 cells. The good performance of the sensor was ascribed to (1) the high sensitivity of the electrochemical technique and (2) two steps for signal amplification. Numerous nucleic acids molecules were attached to the surface of electrode by introducing SNAs AuNPs triggered mimic-HCR amplification. With this amplification, electrochemical signal for telomerase positive cells could be easily distinguished from negative cells even at low cell number and wide detection range. The method presented here was PCR-free, enzyme-free, low cost, simple in operation, and highly sensitive, which make it possible to measure telomerase activity of the cell extract for future clinical use.

AUTHOR INFORMATION

Corresponding Authors

*E-mail: jrzhang@nju.edu.cn.

*E-mail: jjzhu@nju.edu.cn.

Notes

The authors declare no competing financial interest.

ACKNOWLEDGMENTS

We gratefully appreciate the support from National Basic Research Program (Grant 2011CB933502) of China and the National Natural Science Foundation (Grants 21175065, 21375059, and 21335504).

REFERENCES

- (1) Blackburn, E. H. *Cell* **2001**, *106*, 661.
- (2) Harley, C. B.; Futcher, A. B.; Greider, C. W. *Nature* **1990**, *345*, 458.
- (3) Blasco, M. A. *Nat. Rev. Genet.* **2005**, *6*, 611.
- (4) Morin, G. B. *Cell* **1989**, *59*, 521.
- (5) Feng, J.; Funk, W. D.; Wang, S. S.; Weinrich, S. L.; Ailion, A. A.; Chiu, C. P.; Adams, R. R.; Chang, E.; Allsopp, R. C.; Yu, J.; Le, S.; West, M. D.; Harley, C. B.; Andrews, W. H.; Greider, C. W.; Villeponteau, B. *Science* **1995**, *269*, 1236.
- (6) Cohen, S. B.; Graham, M. E.; Lovrecz, G. O.; Bache, N.; Robinson, P. J.; Reddel, R. R. *Science* **2007**, *315*, 1850.
- (7) Shay, J. W.; Bacchetti, S. *Eur. J. Cancer* **1997**, *33*, 787.
- (8) Hiyama, E.; Hiyama, K. *Oncogene* **2002**, *21*, 643.
- (9) Harley, C. B. *Nat. Rev. Cancer* **2008**, *8*, 167.
- (10) Kim, N. W.; Piatyszek, M. A.; Prowse, K. R.; Harley, C. B.; West, M. D.; Ho, P. L. C.; Coviello, G. M.; Wright, W. E.; Weinrich, S. L.; Shay, J. W. *Science* **1994**, *266*, 2011.
- (11) Wright, W. E.; Shay, J. W.; Piatyszek, M. A. *Nucleic Acids Res.* **1995**, *23*, 3794.
- (12) Krupp, G.; Kühne, K.; Tamm, S.; Klapper, W.; Heidorn, K.; Rott, A.; Parwaresch, R. *Nucleic Acids Res.* **1997**, *25*, 919.
- (13) Wege, H.; Chui, M. S.; Le, H. T.; Tran, J. M.; Zern, M. A. *Nucleic Acids Res.* **2003**, *31*, e3.
- (14) Herbert, B. S.; Hochreiter, A. E.; Wright, W. E.; Shay, J. W. *Nat. Protoc.* **2006**, *1*, 1583.
- (15) De Cian, A.; Cristofari, G.; Reichenbach, P.; De Lemos, E.; Monchaud, D.; Teulade-Fichou, M.-P.; Shin-ya, K.; Lacroix, L.; Lingner, J.; Mergny, J.-L. *Proc. Natl. Acad. Sci. U.S.A.* **2007**, *104*, 17347.
- (16) Xiao, Y.; Pavlov, V.; Niazov, T.; Dishon, A.; Kotler, M.; Willner, I. *J. Am. Chem. Soc.* **2003**, *126*, 7430.
- (17) Wang, J. S.; Wu, L.; Ren, J. S.; Qu, X. G. *Small* **2012**, *8*, 259.
- (18) Zhang, Z. X.; Sharon, E.; Freeman, R.; Liu, X. Q.; Willner, I. *Anal. Chem.* **2012**, *84*, 4789.
- (19) Quach, Q. H.; Jung, J.; Kim, H.; Chung, B. H. *Chem. Commun.* **2013**, *49*, 6596.

- (20) Pavlov, V.; Xiao, Y.; Gill, R.; Dishon, A.; Kotler, M.; Willner, I. *Anal. Chem.* **2004**, *76*, 2152.
- (21) Niazov, T.; Pavlov, V.; Xiao, Y.; Gill, R.; Willner, I. *Nano Lett.* **2004**, *4*, 1683.
- (22) Zheng, G. F.; Daniel, W. L.; Mirkin, C. A. *J. Am. Chem. Soc.* **2008**, *130*, 9644.
- (23) Tian, L. L.; Weizmann, Y. *J. Am. Chem. Soc.* **2012**, *135*, 1661.
- (24) Wang, H. B.; Wu, S.; Chu, X.; Yu, R. Q. *Chem. Commun.* **2012**, 48, 5916.
- (25) Maesawa, C.; Inaba, T.; Sato, H.; Iijima, S.; Ishida, K.; Terashima, M.; Sato, R.; Suzuki, M.; Yashima, A.; Ogasawara, S.; Oikawa, H.; Sato, N.; Saito, K.; Masuda, T. *Nucleic Acids Res.* **2003**, *31*, e4.
- (26) Ludlow, A. T.; Robin, J. D.; Sayed, M.; Litterst, C. M.; Shelton, D. N.; Shay, J. W.; Wright, W. E. *Nucleic Acids Res.* **2014**, *42*, e104.
- (27) Sato, S.; Kondo, H.; Nojima, T.; Takenaka, S. *Anal. Chem.* **2005**, *77*, 7304.
- (28) Eskiocak, U.; Ozkan Ariksoysal, D.; Ozsoz, M.; Öktem, H. A. *Anal. Chem.* **2007**, *79*, 8807.
- (29) Yang, W. Q.; Zhu, X.; Liu, Q. D.; Lin, Z. Y.; Qiu, B.; Chen, G. N. *Chem. Commun.* **2011**, *47*, 3129.
- (30) Wu, L.; Wang, J. S.; Ren, J. S.; Qu, X. G. *Adv. Funct. Mater.* **2014**, *24*, 2727.
- (31) Zhang, Z. J.; Wu, L.; Wang, J. S.; Ren, J. S.; Qu, X. G. *Chem. Commun.* **2013**, *49*, 9986.
- (32) Dirks, R. M.; Pierce, N. A. *Proc. Natl. Acad. Sci. U.S.A.* **2004**, *101*, 15275.
- (33) Huang, J.; Wu, Y. R.; Chen, Y.; Zhu, Z.; Yang, X. H.; Yang, C. Y. J.; Wang, K. M.; Tan, W. H. *Angew. Chem., Int. Ed.* **2011**, *50*, 401.
- (34) Ge, Z. L.; Lin, M. H.; Wang, P.; Pei, H.; Yan, J.; Shi, J. Y.; Huang, Q.; He, D. N.; Fan, C. H.; Zuo, X. L. *Anal. Chem.* **2014**, *86*, 2124.
- (35) Huang, J. H.; Gao, X.; Jia, J. J.; Kim, J. K.; Li, Z. G. *Anal. Chem.* **2014**, *86*, 3209.
- (36) Zhang, B.; Liu, B. Q.; Tang, D. P.; Niessner, R.; Chen, G. N.; Knopp, D. *Anal. Chem.* **2012**, *84*, 5392.
- (37) Choi, J.; Routenberg Love, K.; Gong, Y.; Gierahn, T. M.; Love, J. C. *Anal. Chem.* **2011**, *83*, 6890.
- (38) Taton, T. A.; Mirkin, C. A.; Letsinger, R. L. *Science* **2000**, *289*, 1757.
- (39) Zhang, J.; Song, S. P.; Zhang, L. Y.; Wang, L. H.; Wu, H. P.; Pan, D.; Fan, C. H. *J. Am. Chem. Soc.* **2006**, *128*, 8575.
- (40) Liu, J. W.; Lu, Y. *Nat. Protoc.* **2006**, *1*, 246.
- (41) Zheng, J.; Zhu, G. Z.; Li, Y. H.; Li, C. M.; You, M. X.; Chen, T.; Song, E. Q.; Yang, R. H.; Tan, W. H. *ACS Nano* **2013**, *7*, 6545.
- (42) Wang, J. S.; Wu, L.; Ren, J. S.; Qu, X. G. *Nanoscale* **2014**, *6*, 1661.